ASSESSMENT OF THE SOLAR RADIATION POTENTIAL OF THE THIKA AND NAIROBI AREA

N. W. Wasike[1], T.N. Soitah[2], S. M. Waweru[3] and F. N. Kariuki[4]
[1,2,3,4] Physics Department, Jomo Kenyatta University of Agriculture and Technology, Nairobi, Kenya
E-mail: nahashonwasike@gmail.com

Abstract
This assessment seeks to provide information on the solar energy resource potential of the Thika – Nairobi area essential in the dissemination of Renewable Energy Technologies which are essentially solar photovoltaic and thermal systems. To achieve this, solar radiation data for three stations (Dagoretti Corner, Thika and Jomo Kenyatta International Airport (JKIA) has been collected and analyzed with the aim of assessing the solar radiation potential. The Thika station is at an altitude of 1500 m above sea level and located at (0°, 37° 41' East). Dagoretti Corner station is at 1795 m above sea level and at (01° 18' S, 36° 45' E). The JKIA station is at 1624 m above sea level and at (1° 19’ S, 36° 55' E). The longitudinal and latitudinal difference between these stations is small and that shows how close the stations are to one another. This facilitated the ease of comparison and categorization of the two regions. Data was collected using two instruments: the Gunn – Bellani and the pyranometer. The Gunn – Bellani registers radiation in terms of the amount of liquid distilled, whereas the pyranometer used registers solar radiation in terms of counts. The raw data was first converted to MJ/m^2/day and then subjected to quality control procedures. After quality control procedures, the data was analyzed in terms of the average monthly daily insolation. Extraterrestrial solar radiation was estimated using an empirical formula and by using the values of the extraterrestrial solar radiation values of parameters like diffuse solar radiation and clearness index were calculated. Statistical parameters e.g. standard deviation, Skewness and coefficient of variation, were calculated using software to show the variability in the solar energy resource. The analysis shows that the study area has reliable solar energy resources with little variability. The average monthly daily insolation ranges from 3 kWh/m^2/day to 7 kWh/m^2/day. The national average of 4 – 6 kWh/m^2/day from earlier studies falls within this range. The transparency of the sky estimated by the formula $K_T = \frac{H}{H_0}$ is also encouraging as it shows that there is little obstruction to the solar radiation. Diffuse solar radiation levels are also high and this shows that incase of obstruction, the diffuse solar radiation can be relied on. The abundance of the resource shows that it is feasible for applications of both solar photovoltaic technologies and solar thermal technologies.

Key words: Insolation, declination, extraterrestrial, photovoltaics

1.0 Introduction

Rising prices of petroleum/oil products, their high rate of depletion, high population growth and rapid development call for alternative sources of energy. Renewable energy is considered a key source of energy for the future. In Kenya, the ministry of energy specifies that despite the fact that the country is endowed with significant amounts of renewable energy resources which include wind, biomass, solar, geothermal and small hydro; few renewable energy resources in the country have been fully assessed, mapped and appraised for their technical and economic viability (Ministry of Energy, (MoE), 2002). The ministry went further and highlighted solar energy as one of the alternative forms of energy that should be developed in rural areas. This source of energy has not been fully utilized in Kenya due to a number of factors, including relative high costs of systems and lack of standards.

Several studies have been conducted to ascertain the potential of solar. To highlight a few, Barman (2011), in his analysis gave the annual insolation of Nairobi as 2,100 kWh/m^2. Okoola (1982) observed that insolation increases from zero at sun rise and reaches its peak in the early afternoon (solar noon). The energy then reduces in intensity until it reaches zero after sunset. Newham *et al.*, (1983) outlined that the country's average solar insolation was 5.5 kWh/m^2/day.

Ogallo and Runanu (1989) in their study delineated the country into several homogenous solar energy zones forming a good basis for the planning of solar systems investment in the country. Hankins, (1991), specified that the country receives an average solar radiation of 700 W/m^2 and mean sunshine duration of 8 hours and hence viable for both solar photovoltaics (PVs) and solar thermal systems. Marigi (1999), showed that the mean solar values never exceed 972 Wh/m^2 and the values measured on the horizontal surface are greater in lowlands than those in highland areas. Most of the earlier studies concentrated on global solar radiation without putting in consideration, the contribution of the diffuse solar radiation and the variation in the transparency of the sky. It should also be clear that earlier researchers concentrated in Nairobi. Comparing Nairobi's insolation to areas close or rather within the Nairobi metropolitan region will offer useful information in the dissemination of the renewable energy technologies.

This study aims at evaluating the insolation available in the Thika and Nairobi area for the purpose of solar panel sizing and costing. It puts into consideration the contribution of the diffuse solar radiation. The variation of the transparency of the sky will also be calculated. Therefore this analysis recognizes the fact that a detailed knowledge of solar radiation is essential for its successful application. A higher solar radiation potential sustains the performance of solar photovoltaic and thermal systems.

2.0 Methodology

2.1 Procedure/Data Collection

The instruments used in the data collection of the data were the pyranometer and the Gunn-Bellani. The pyranometer measures both global and diffuse solar radiation while the Gunn – Bellani can only measures global solar radiation. The pyranometer registers radiation in radiations counts. To convert counts to solar energy in terms of MJ/m^2, the following relation was be used:

$$\text{Solar energy}(MJ/m^2)=R\times L \quad \ldots\ldots\ldots\ldots\ldots\ldots\ldots\ldots\ldots\ldots\ldots\ldots \quad (1)$$

Where R is the amount of radiation in terms of counts and L is the instrument constant given by L=1.022$\times 10^{-3}$ MJ/m^2/count.

The Gunn – Bellani registers radiation in terms of the amount of liquid distilled. Using a calibration formula:

$$R = Ad + B \quad \ldots\ldots\ldots\ldots\ldots\ldots\ldots\ldots\ldots\ldots\ldots\ldots\ldots\ldots\ldots\ldots \quad (2)$$

where:

R = radiation intensity in cal/cm^2/day.

d = amount of water distilled in ml

and A and B are calibration constants.

The radiation registered in form of distillate was converted to cal/cm^2/day. The radiation in cal/cm^2/day was converted to MJ/m^2 by multiplying by a factor of 0.042791 MJ/m^2/day per cal/cm^2/day (Mwebesa, 1980).

2.2 Prediction of Diffuse Solar Radiation (H_d)

The diffuse solar radiation H_d was estimated by the empirical formula below:

$$\frac{H_d}{H} = 1.00 - 1.13K_T \quad \ldots\ldots\ldots\ldots\ldots\ldots\ldots\ldots\ldots\ldots\ldots\ldots\ldots\ldots\ldots\ldots \quad (3)$$

Where H_d is the mean of the daily diffuse solar radiation and K_T is the clearness index (also referred to as the sky transmissivity). The other correlation equation for estimating diffuse solar radiation is given as:

$$\frac{H_d}{H} = 1.390 - 4.027K_T + 5.53(K_T)^2 - 3.108(K_T)^3 \quad \ldots\ldots \quad (4)$$

In this analysis, the correlation equation the first correlation equation (eq. 1) was used. Clearness index (K_T) was estimated by:

$$K_T = H/H_0 \quad \ldots\ldots\ldots\ldots\ldots\ldots\ldots\ldots\ldots\ldots\ldots\ldots\ldots\ldots\ldots\ldots \quad (5)$$

where H is the global solar radiation and H_0 is the extraterrestrial insolation. The extraterrestrial solar radiation on a horizontal surface was calculated using the equation below.

$$H_0 = \frac{24\times 3{,}600}{\pi} I_{sc}\left[1 + 0.033\cos\left[360\frac{dn}{365}\right]\right]\left[\left[\frac{2\pi\omega_s}{360}\right]\sin\phi\sin\delta + \cos\phi\cos\delta\sin\omega_s\right] \quad (1)$$

where I_{sc} is the solar constant equal to 1367 Wm^{-2}.

ω_s is the hour angle for horizontal surface and is estimated by:

$$\omega_s = \cos^{-1}(-\tan\phi \tan\delta) \quad \text{.....} \quad (2)$$

ϕ is the latitude and it is taken to be positive for the northern hemisphere and negative for latitude in the southern hemisphere.

δ is the declination and is calculated using the formulae below

$$\delta = 23.45 \sin\left[360\frac{284+\mathrm{dn}}{365}\right] \quad \text{.....} \quad (3)$$

Where dn is the day of the year from January 1st to December 31st. (Ahmed *et. al*, 2009)

2.3 Theoretical Modeling of Solar Insolation

Annandale (2002) modified the Hargreaves and Samani model of "(1982)" and gave it as below:

$$\mathrm{T_t} = \kappa_{\mathcal{H}}(1 + 2.7 \times 10^{-5} Alt)\sqrt{\Delta \mathrm{T}} \quad \text{.....} \quad (6)$$

Where $\sqrt{\Delta \mathrm{T}}$ is the square root of the difference in temperature i.e the maximum and minimum temperature. Annandale specified that the value for $\kappa_{\mathcal{H}}$ should be 0.19 for coastal regions and 0.16 for inland regions, which were the same values that had been specified by Hargreaves and Samani. The coefficient 2.7×10^{-5} takes care of the reduced atmospheric height and *Alt* is the altitude and these are the two factors that were added by Annandale. $\mathrm{T_t}$ is the sky transmissivity which is given by:

$$\frac{\mathrm{H}}{\mathrm{H_0}} = \mathrm{T_t} \quad \text{.....} \quad (7)$$

2.4 Quality Control of Data

Before applying eq.7, the coefficient k_H, complete data sets from the three stations were used to validate the value. From the average values, it was found that the value obtained agrees with the value that was given by Hargreaves and Samani. The missing data sets were then estimated using eq.7. The collected data was subjected to quality control procedures that included physical scanning of the data, the mass curve analysis and use of the box plot. Erroneous data (the data that fall outside the required limits) were identified and corrected. The box plot outlines the outliers in two ways. One is outliers that are within the normal range and second the extreme outliers. Extreme outliers were the ones considered for correction. Quality control procedures therefore ensured that the data was within the required logical and physical limits.

2.5 Measures of Dispersion

Measures of dispersion generally quantify the general spread of the observed solar energy values about the mean (normal expectations). This information is essential if the available solar energy resources were to be effectively tapped for continuous applications and planning of supplementary energy resources. The most commonly used measures of dispersion include the coefficient of variation (δ_v), relative mean linear successive difference (δ_d), skewness coefficient, kurtosis coefficient and

higher order moments. Of interest in this assessment is the coefficient of variation which cannot be estimated without the value of the standard deviation. Some of the useful equations for determining these quantities are given below:

$$\text{Average/mean} = \frac{\sum fx}{\sum f} \quad (1)$$

$$\text{Standard deviation } (\sigma) = \sqrt{\frac{\sum fx^2}{N} - (\bar{x})^2} \quad (2)$$

$$\text{Coefficient of variation } (\delta_v) = \frac{\sigma}{\bar{X}} \times 100 \quad (3)$$

3.0 Results

After manipulation of the data, this section presents the results of the data assessment. The results are presented in terms of monthly radiation trends, monthly trend in diffuse radiation, average monthly contribution of the diffuse solar radiation to global solar radiation and monthly variation in the clearness index.

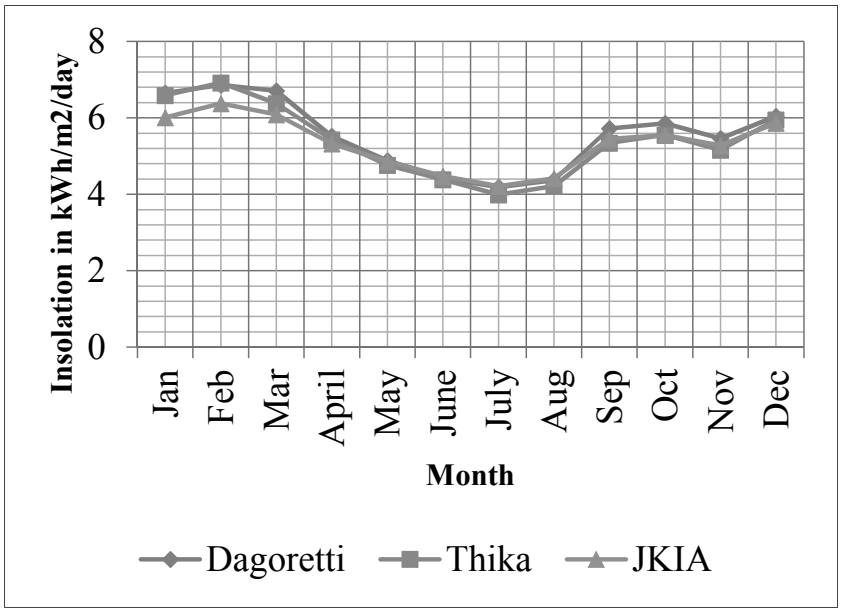

Figure 2: Monthly variability in global solar radiation for Dagoretti Corner, Thika and JKIA

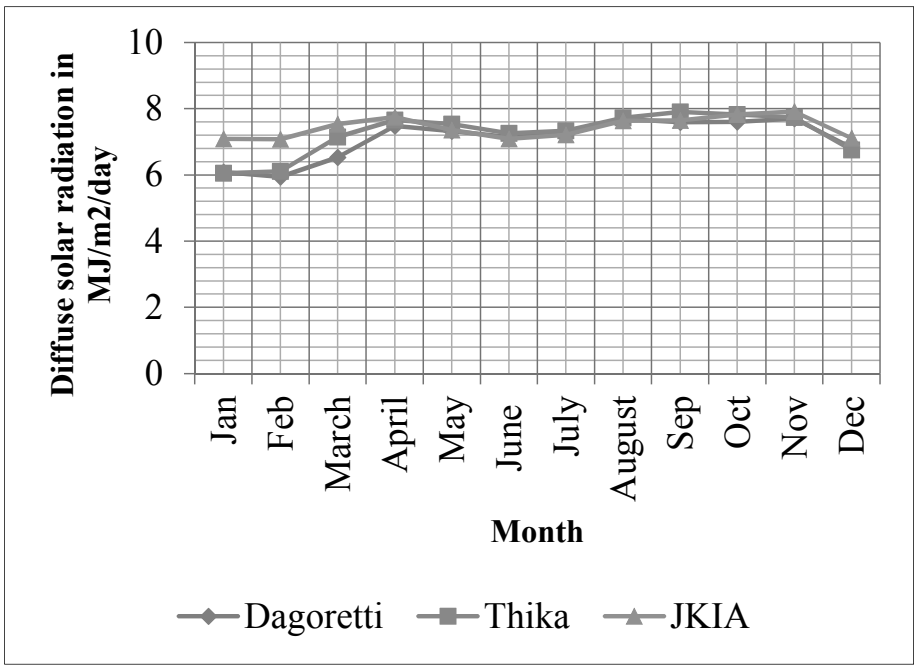

Figure 3: Monthly variability in diffuse solar radiation for Dagoretti Corner, Thika and JKIA

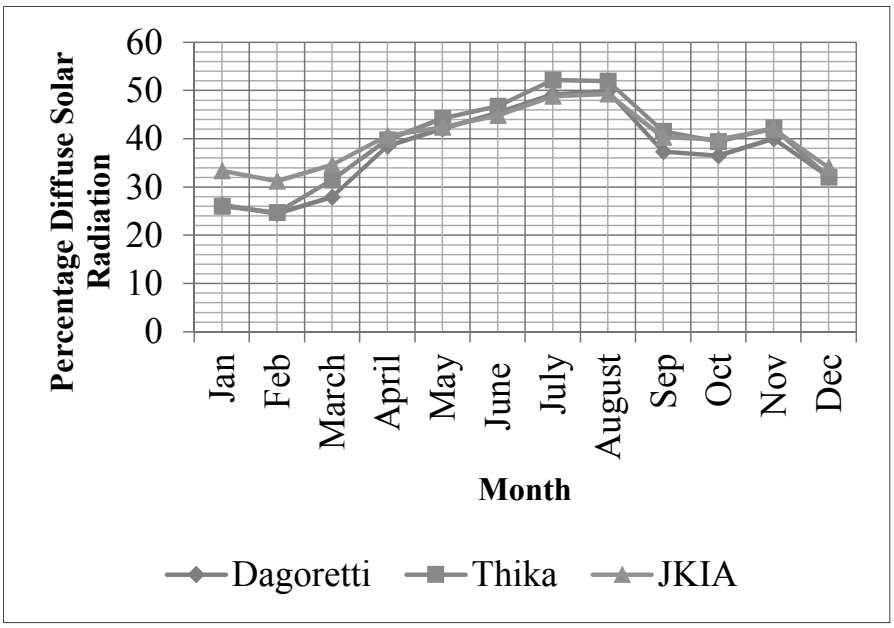

Figure 4: Average monthly percentage contribution of diffuse solar radiation trend for Dagoretti Corner, Thika and JKIA

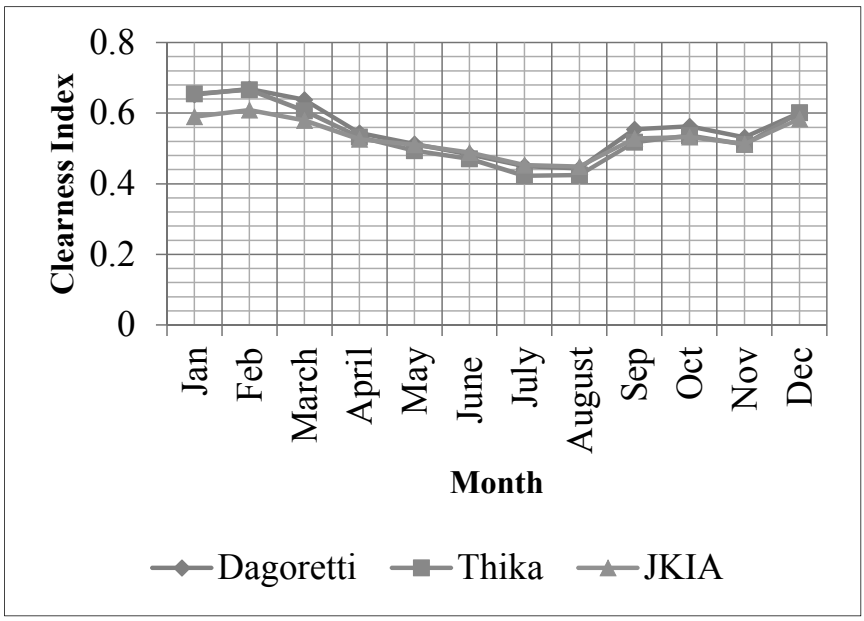

Figure 5: Average monthly clearness index for Dagoretti Corner, Thika and JKIA

3.1 Monthly Radiation Trends

Fig. 1 represents the monthly trends in global solar radiation at Dagoretti corner, Thika and JKIA stations respectively. From the figure, it can be seen from the three curves that global solar radiation reaching these regions increases in intensity from January and reaches its peak value in February. Despite the intensity being high in March, it starts to decrease, a process that continues in the follow up months reaching the lowest intensity in July. The radiation intensity then starts increasing again in August through September and reaches another peak in October. This peak is lower than the one in February. We also observe that the intensity slightly reduces in November and then increases during the month of December.

3.2 Monthly Trend In Diffuse Solar Radiation

Fig. 2 represents the monthly variation in diffuse solar radiation. The curves show that the first peak diffuse solar radiation is observed in April for all the stations. Dagoretti Corner's other peaks are seen in August and November. Thika station has peaks in September and November while JKIA has only one other peak in October though the radiation in November is still high.

3.3 Average Monthly Contribution of Diffuse Solar Radiation to Global Solar Radiation

From the curves in Fig. 3 it can be noted that the maximum contribution of diffuse solar radiation to the global solar radiation is received between June and September. Dagoretti Corner has the maximum contribution falling in the month of August; Thika and JKIA have their maximum contribution in July.

Generally, the diffuse solar radiation increases in intensity from a minimum in February to a maximum in either July or August. The intensity then reduces through October. It increases slightly in November and then decreases through January.

3.4 Monthly Variation in the Clearness Index

Fig. 4 presents the monthly trend/variation in the clearness index. From the figure, the clearness index is peak in February; it then reduces to its minimum in August. August lies in the cold season while February falls in the dry season. From August, the clearness index increases as the amount of obstruction to the incoming solar radiation reduces but with the short rains, it can be seen that in November, the index reduces slightly before increasing again in December.

3.5 Analysis of the Results

Fig. 5 below is a presentation of the results of the insolation at the Dagoretti corner station using the box plot. The box plot gives the mean, median and the outliers. As seen on the graph, the two data points below the curve represent the outliers. Other graphs had these data points above and below the curve. It also shows whether the distribution is either positively or negatively skewed. Similar representations were also done for insolation at Thika and JKIA stations. The box plot was extended to the other parameters i.e. diffuse solar radiation, percentage diffuse solar radiation and the clearness index.

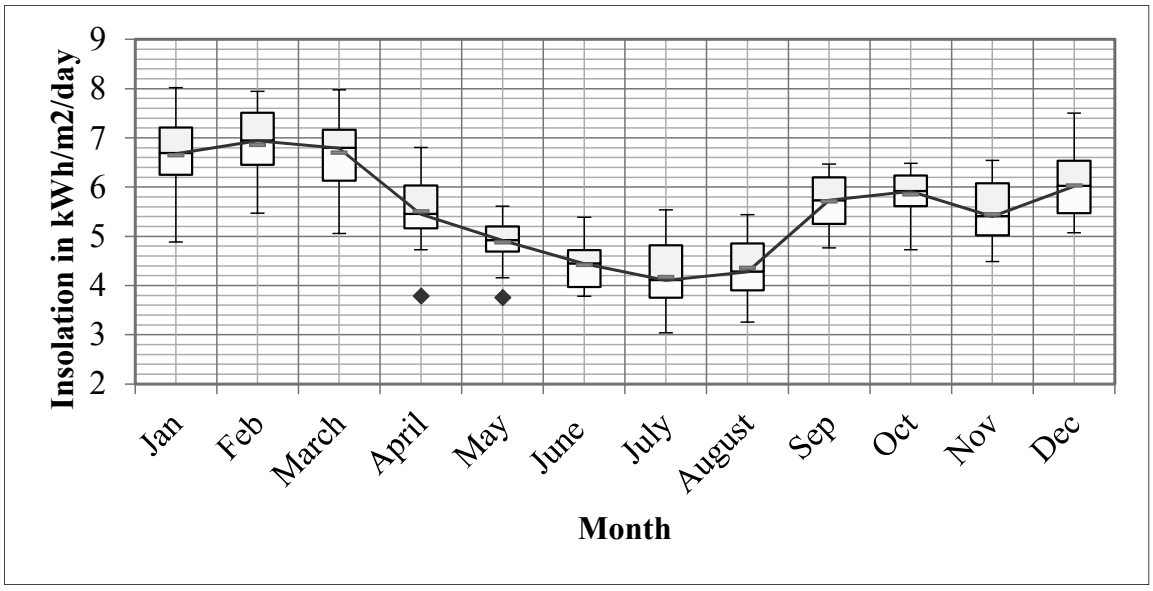

Figure 6: Monthly insolation trend at Dagoretti Corner using the box plot

Using excel, the whole set of data was selected and subjected to a scan. Those points which the software outlines as the outliers were counted. As a fraction of the total data items, errors in the calculation/estimation of the various parameters are determined

The statistical parameters were calculated using an Excel add in called SCC stat. In this assessment, the coefficient of variation (δ_v) was put into consideration. Values of $\delta_v > 1$ reflect cases where the standard deviation is greater than the mean expectation. The larger the δ_v values reflect higher degree of variability in the available solar power potential. Higher variability degrees quantify the higher degree of unreliability of the available solar power (Marigi, 1999).
All the values of δ_v were found to be less than 1, which shows that there is a low degree of variability and hence a high degree of reliability.
Other than the use of software, equations 11, 12 and 13 could also be used in the calculation of the mean, standard deviation and the coefficient of variation.

4.0 Discussion

Peak radiation in the month of February between 6 – 7.5 kWh/m^2/day and sometimes as high 8 kWh/m^2/day is attributed to the season being generally dry and less windy. This month is the climax of the dry seasons which runs all the way from December. March marks the onset of the long rains season as well as the downward trend in the insolation. The rains begin in mid – March and ran through to May. April therefore is the climax of the long rains. The long rains season is characterized by the heavy clouds which adversely affect the amount of radiation received during this season. The heavy clouds therefore obstruct much of the beam radiation and hence more of the diffuse radiation is received.

The cold season starts in June and runs through to August. The lowest insolation level of between 3 kWh/m^2/day and 5kWh/m^2/day for all the three stations is registered in this season. The season is normally characterized by lower tropospheric clouds (stratiform type) that are convectively stable coupled with low level temperature inversions especially over the highlands. The clouds obstruct of the beam radiation with much of it either absorbed by the water droplets or reflected back into the sky. In effect this causes July to have the least insolation.
September to November is the short rains period. The season is associated with abundant moisture, cloudiness and rainfall. Most of the short rains fall in the month of October, November and December (OND). From the curves in Fig. 1, lower insolation is experienced in October and November. The insolation is higher than in insolation in July which shows that the amount of obstruction to the radiation is lower than in July.

The curves in Fig. 2 show an inverse relation to the curves Fig. 1. The least diffuse solar radiation was recorded in February while the maximum insolation is recorded in the same month. Therefore with the dry conditions, the sky is more transparent. With little moisture suspended in the sky little amount of radiation is absorbed and also with reduced aerosol concentration in the sky little scattering is experienced and hence less diffuse solar radiation is received. More beam radiation reaches the ground and in effect more insolation is registered. One major characteristic of the

month of April, August, October and November is the cloudiness, which obstruct the beam radiation and contribute to the higher values of diffuse solar radiation. Part of the beam radiation from the sun is absorbed and scattered and therefore less beam radiation is received in the long rains season, cold season and the short rains period. From Fig. 4, the clearness index (the transparency of the sky to the oncoming solar radiation) follows the same pattern as the insolation trend. The least clearness index of < 0.5 was recorded in July being a month that falls in the cold season. The cloudiness in this month affects the transparency of the sky. The clouds obstruct the beam radiation affecting the amount of insolation received. Lower clearness index in November is attributed to cloudiness in this month. Higher indices in the month of December, January and February are attributed to the season being dry with little obstruction to the beam radiation.

The rainfall patterns are controlled by the migration of the Inter – Tropical Convergence Zone (ITCZ) which is a relatively narrow belt of very low pressure and heavy precipitation that forms near the earth's equator. It migrates southwards through Kenya in October to December, and returns northwards in march, April and May. This causes Kenya to experience short rains in October to December and long rains in March to May.

From Fig. 1, it can be seen that Dagoretti corner has an average monthly daily insolation ranges from 4 kWh/m^2/day to 7 kWh/m^2/day. For Thika, the average monthly daily insolation ranges from 3.8 kWh/m^2/day to 7 kWh/m^2/day and for JKIA, it ranges from 3.8 kWh/m^2/day to 6.4 kWh/m^2/day. This shows that the solar energy resources are quite substantial. These results agree with the value obtained by Klaus *et al.*, (1990). The results also show that that the national average of 4 – 6 kWh/m^2/day given by MoE 2004 and 2011, Aurela (2012) and Hille (2011) fall within the range. The same range of insolation is highlighted in the energypedia.info. Karakezi *et.al.* (2006) specified that the country's average annual daily insolation is 6.0 kWh/m^2/day. This average falls within the average arrived at in this study. Gichungi (2012) highlighted the national average as 4.5 kWh/m^2/day. This results fall short of the expected results despite the fact that it falls within the results obtained in this analysis. Solar and Wind Energy Resource Assessment (SWERA) report of 2008, shows that the average annual daily insolation in the study area ranges from 4.5 – 4.75 kWh/m^2/day which falls in the range arrived at in this analysis.

Baanabe *et.al.* (2008) specify that all the countries in the East and Horn of Africa region enjoy long sunshine hours and have a daily average solar insolation of about 4.5–6.5 kWh/m^2. This result agree with the finding in this analysis.
Apart from the climatic conditions, the other factors affecting the solar radiation received are: the distance from the sun, geographical location (in terms of latitude

and longitude), the local landscape, time of the year, time of the day and solar elevation or inclinations of the solar rays in the horizon (Marigi, 1999).

5.0 Conclusion

From the analysis it can be concluded that the Thika – Nairobi area has reliable solar energy resources. Minimum insolation falls in the cold season of June – August and maximum insolation is usually recorded in the dry season of December to February. The average monthly daily insolation ranges from 3 – 7 kWh/m^2/day. The contribution of the diffuse solar radiation is enormous. This shows that in the absence of the beam radiation, the diffuse solar radiation can be made use of. The transparency of the sky is encouraging with little obstruction to the incoming solar radiation. These resources call for the application of the renewable radiation technologies in solar radiation.

Acknowledgement

The auhor expresses sincere gratitude to the Kenya Meteorological Department for assistance offered. I would also like to thank their staff for the valuable information they provided. We wish to thank the National Council for Science and Technology (NCST) for financial support and finally I would to thank the Physics Department , JKUAT for help and support.

References

Ahmed M. A., Ahmad F., Akhtar M. W. (2009), *Estimation of Global and Diffuse Solar Radiation for Hyderabad, Sindh, Pakistan*, Journal of Basic and Applied Sciences Vol. **5(2)**, 73-77, Karachi, Pakistan.

Annandale J.G., Jovanic N.Z., Benade N., Allen R.G. (2002), *Software for missing data error analysis Penman–Monteith reference evapotranspiration,* Irrig. Sci., **21**, 57–67.

Aurela B. (2012), *Kenya & Renewable Energy – Country at-a-glance*, Federation of Universities of Applied Sciences, Helsinki – Finland.

Baanabe J., Mwihava, N. and Kiva. D. (2008), *Large Scale Hydropower, Renewable Energy Adaptation &Climate Change &Energy Security in East &Horn of Africa*: A paper presented at HBF Regional Workshop on 21st November, 2008

Barman J. (2011), *Design and Feasibility study of PV systems in Kenya,* Master's Thesis within Sustainable Energy System programme, Chalmers University of Technology, Göteborg, Sweden.

Georg H., Dieter S., Hermann L., Eberhard R., Kilian R.,(2012), *Grid Connection of Solar PV. Technical and Economic Assessment of Net-Metering in Kenya.* Deutsche Gesellschaft für Internationale Zusammenarbeit (GIZ), Berlin, Germany, pp. 9 -12.

Gichungi H.(2012), *Solar Potential in Kenya*, MoE, Nairobi – Kenya.

Hankins M. (1991), *Renewable Energy in Kenya,* Motif Creative Arts, Nairobi

Hargreaves G.H., Samani Z.A., (1982), *Estimating Potential Evapotranspiration*, J. Irrig. Drain. E. ASCE,**108**, pp. 225–230.

Karekezi S., Kithyoma W., Wangeci J., Gashie W., Turyahabwe E., Onguru O., Balla P. and Ochieng X. (2006), *The Potential of Small and Medium-Scale Renewables in Poverty Reduction in Africa*, Nairobi, AFREPREN/FWD and Heinrich Boll Foundation (HBF)

Klaus K., Marianne R., Detlef S. (1990), *Solar Cookers in the Third World,* Deutsche Gesellschaft für Technische Zusammenarbeit (GTZ) GmbH, Berlin, Germany.

Klein S. A. (1977), *Calculation of Monthly Average insolation on Tilted Surface. Solar Energy.* 9: 325.

Marigi S. N. (1999), *An assessment of Solar Energy Resources in Kenya,* PhD Thesis, Moi University-Kenya.

MoE (2002), *Study on Kenya's Energy Demand, Supply and Policy Strategy for Households, Small Scale Industries and Service Establishments – final Report – September 2002*, Kamfor Company limited, Nairobi.

MoE (2004), *National Energy Policy,* Sessional Paper No. 4, MoE- Nairobi.

MoE (2011), *Scaling-Up Renewable Energy Program (SREP),* MoE-Nairobi.

Mwebesa M. N. M (1980), *Handbook of Meteorological Instruments,* Kenya meteorological department - Nairobi.

Newham N. (1983), *Can Solar Energy Replace Wood and Oil Fuels in Kenya's Commercial and Industrial Sectors?* World Solar Power Foundation- Nairobi.

Ogallo L. and Runanu K. (1989), *Space Time Characteristics of the Maximum and Minimum Solar Power Expectations in Kenya,* First National Conference on Met. Applications, Nairobi - Kenya.

Okoola R.E. (1982), *Solar Power Potential in Kenya,* An IMTR Research Publication report. No. 1/82.

Thueri D. (2008), *Solar and Wind Energy Resource Assessment,* UNEP/DTIE, Nairobi.